

## Stochastic broadening and magnetic footprints from the magnetic noise and field errors in the DIII-D tokamak

Alkesh Punjabi<sup>1</sup> and Halima Ali<sup>1</sup>

<sup>1</sup>*Hampton University, Hampton, Virginia 23668, USA*

**Abstract:** The Grad-Shafranov solver code EFIT data for the shot 115467 at 3000 ms in the DIII-D tokamak is used to construct the equilibrium poloidal magnetic flux  $\chi(\psi, \theta)$ .  $\psi$  is the toroidal magnetic flux, and  $\theta$  is the poloidal angle.  $\chi$  is the Hamiltonian for the trajectories of magnetic field lines,  $\theta$  is the canonical position,  $\psi$  is the canonical momentum, and the toroidal angle  $\phi$  is the canonical time. The equilibrium Hamiltonian for the DIII-D that we have constructed represents the magnetic topology and the magnetic geometry of the DIII-D very accurately [1,2]. We use the equilibrium poloidal flux as the generating function, and construct a symplectic map for the trajectory of field lines in the DIII-D in natural canonical coordinates. The natural canonical coordinates can be inverted to physical space [1,2]. We use the map to calculate the stochastic broadening of the separatrix in the DIII-D from noise and error fields. We use the continuous analog of the map to calculate the magnetic footprint in the DIII-D from noise and error fields. We estimate the scaling of the width of stochastic layer and the area of footprint with strength of the noise and error fields. The results of this study will be presented.

Recently we have developed a new set of canonical coordinates for symplectic integration of magnetic field lines in divertor tokamaks [1,2]. These new coordinates are called natural canonical coordinates. The advantage of these new coordinates are that they can be readily inverted to physical coordinates ( $R, Z$ ), and the trajectories can be integrated across the separatrix surface, and the symplectic map in these coordinates does not distort the equilibrium surfaces as the surfaces advance toroidally. The new coordinates are  $(\psi, \theta, \phi)$ .  $\psi$  is the canonical momentum,  $\theta$  is the canonical position, and  $\phi$  is the canonical time. Poloidal magnetic flux,  $\chi(\psi, \theta, \phi)$ , is the Hamiltonian, and it is expressed as  $\chi(\psi, \theta, \phi) = \chi_0(\psi, \theta) + \chi_1(\psi, \theta, \phi)$ , where  $\chi_0(\psi, \theta)$  is the equilibrium, axisymmetric Hamiltonian given by

$$\chi_0(u(\psi, \theta), v(\psi, \theta)) = \sum_{i=1}^5 a_i u^i + \sum_{j=1}^6 b_j u^j + \sum_{\substack{i=1,5 \\ j=1,6}} c_{ij} u^i v^j.$$

The coefficients  $a_i$ ,  $b_j$ , and  $c_{ij}$  are determined from the Grad-Shafranov equilibrium data [3] for the shot 115467 at 3000 ms in the DIII-D. The equilibrium magnetic surfaces constructed from the equilibrium Hamiltonian give a very accurate and very realistic representation of the magnetic surfaces, their geometry, and topology in the shot 115467 at 3000 ms. A canonical transformation in the new coordinates gives the symplectic map for the field line trajectories

in the shot. The map equations in the new coordinates are  $\psi_{n+1} = \psi_n - k \frac{\partial \chi(\psi, \theta, \phi)}{\partial \theta_n}$ ,

and  $\theta_{n+1} = \theta_n + k \frac{\partial \chi(\psi, \theta, \phi)}{\partial \psi_{n+1}}$ . The topological noise and field errors magnetic perturbation for

the DIII-D [4,5] is chosen to be  $\chi_i(\theta, \phi) = \delta \sum_{(m,n)} \cos(m\theta - n\phi)$ , with  $(m,n) = \{(3,1), (4,1), (6,2),$

$(7,2), (8,2), (9,3), (10,3), (11,3)\}$ . The step size of the map is  $2\pi/360$ . We start field lines on the line joining the O-point to X-point,  $\theta_0 = \theta_X$ , and  $\phi_0 = 0$ .  $\theta_X = 4.28$  radians is the poloidal position of the X-point in the DIII-D. We advance each line for at most  $10^5$  toroidal circuits of the DIII-D. If a field line crosses the plane  $Z - Z_0 = -0.75$  m before completing  $10^5$  toroidal circuits, we consider it to be chaotic; otherwise we consider it to be nonchaotic.  $(R_0, Z_0)$  is the O-point in the DIII-D shot. We calculate trajectories of 150 field lines. Lines start at intervals separated radially by a distance of 1 mm. We calculate the width of stochastic layer in the DIII-D for  $8 \times 10^{-6} \leq \delta \leq 2 \times 10^{-5}$ . See Fig. 1.

The width of stochastic layer,  $w(\delta)$  varies from 5.7 mm to 11.6 mm. A power fit shows that the width scales as  $\delta^{0.56}$ . The scaling of width with amplitude deviates from the Boozer-Rechester prediction [6] by 12%.  $\delta = 2 \times 10^{-5}$  is the correct  $\delta$  for DIII-D field-errors and it is about the same size as the  $n=3$  I-coil perturbation that was applied to get ELM suppression in this plasma [7]. The poloidal flux loss from the stochastic layer varies from 0.2 to 0.9% of the poloidal flux inside the ideal separatrix. See Fig. 2. The area of footprint A varies from  $1 \times 10^{-3}$  m<sup>2</sup> to  $3 \times 10^{-3}$  m<sup>2</sup>. The area scales linearly with  $\delta$ . See Fig. 2. See Fig. 3. The fractal dimension varies from 1.36 to 1.65. Fractal dimension scales as  $\delta^{-1/5}$ . See Fig. 4. The radial field diffusion coefficient  $D_F$  near the X-point for the lines that strike the plate varies from  $2.37 \times 10^{-5}$  to  $2.62 \times 10^{-5}$  m<sup>2</sup>/radian (of toroidal rotation). The average distance traveled by field lines that strike the plate,  $\langle L \rangle_{\text{strike}}$ , is about 450 to 600 m. See Figs. 5 and 6. The inboard footprint is in the shape of three winding toroidal stripes. See Fig. 7. The footprint in the variables  $\zeta = \Delta Z \cos(\phi_s)$  and  $\eta = \Delta Z \sin(\phi_s)$  are shown in Fig. 8.

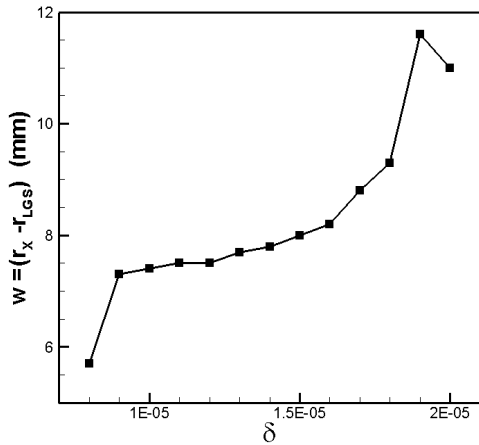


Fig. 1. Width of stochastic layer in the DIII-D.

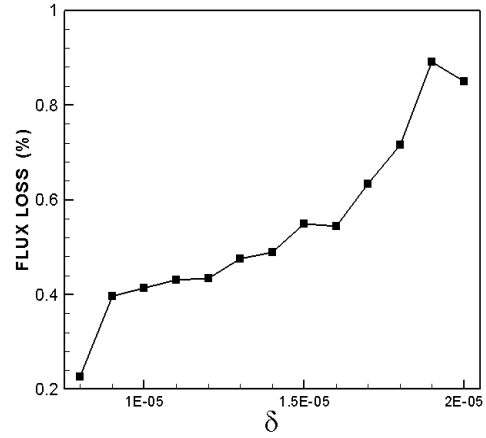


Fig. 2. Poloidal flux loss in the DIII-D.

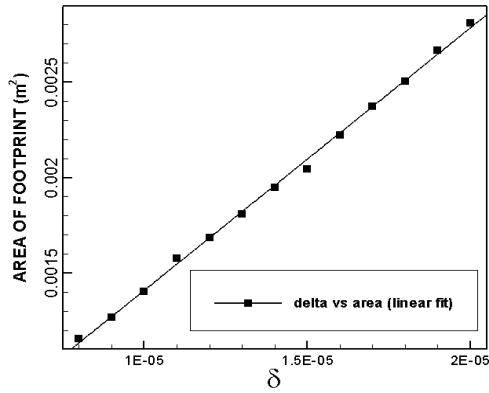
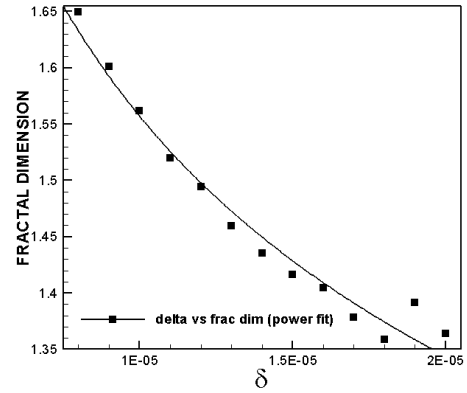
Fig. 3. Scaling of area of footprint with  $\delta$ .

Fig. 4. Scaling of the fractal dimension of the footprint.

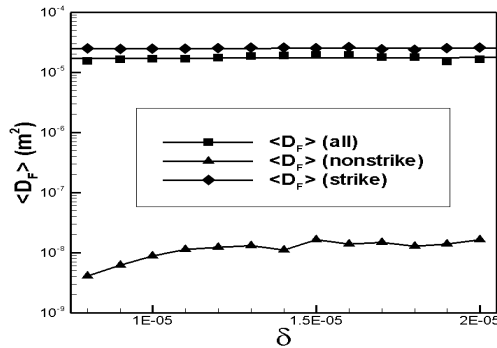


Fig. 5. Average field diffusion coefficient for the lines that strike the inboard plate in the DIII-D.

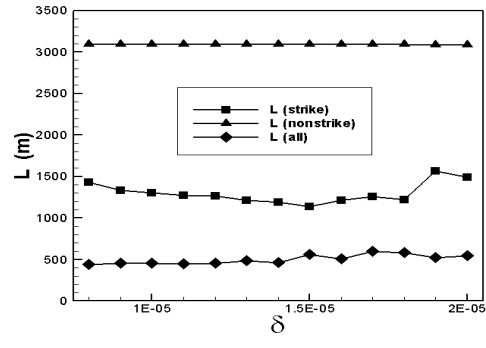


Fig. 6. Average length of field lines in the DIII-D.

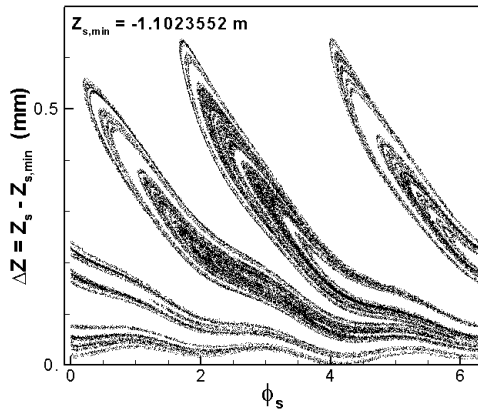


Fig. 7. Inboard magnetic footprint in the DIII-D for  $\delta=8\times 10^{-6}$ .

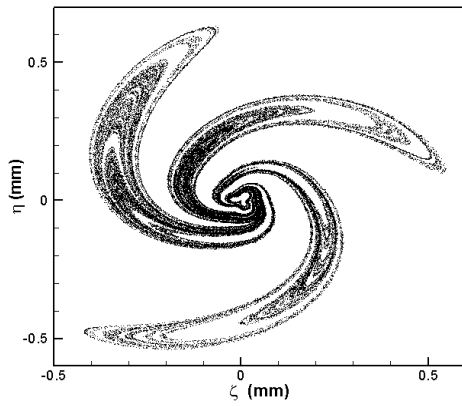


Fig. 8. Inboard magnetic footprint in the DIII-D for  $\delta=8\times 10^{-6}$  in the  $(\zeta, \eta)$  coordinates.

The footprints are calculated using the continuous analog of the discrete map. The physical parameters of the footprint, such as strike angles, lengths, safety factor, and radial diffusion, show a fractal structure. These are the preliminary results of our work. Detailed results will be analyzed and reported in a regular paper.

Authors thank Dr. Allen Boozer and Dr. Todd Evans for useful discussions and comments. This work is supported by grants DE-FG02-01ER54624 and DE-FG02-04ER54793. This research used resources of the NERSC, supported by the Office of Science, US DOE, under Contract No. DE-AC02-05CH11231.

## References

- [1] A. Punjabi, *Nucl. Fusion* **49**, 115020 (2009).
- [2] A. Punjabi and H. Ali, *Phys. Plasmas* **15**, 122502 (2008).
- [3] Lao L. et al 2005 *Fusion Sci. Technol.* **48** 968.
- [4] J. L. Luxon et al, *Nucl. Fusion* **43**, 1813 (2003).
- [5] T. E. Evans 1991, EPS, Petit-Lancy, Part II, p. 65.
- [6] A. Boozer and A. Rechester, *Phys. Fluids* **21**, 682 (1978).
- [7] T. E. Evans et al, *Phys. Rev. Lett.* **92**, 235003 (2004).